

Physiological Research Pre-Press Article

1 Title: Intra-articular injection of mitomycin C prevents progression of immobilization-
2 induced arthrogenic contracture in the remobilized rat knee

3

4 Akinori Kaneguchi¹, Junya Ozawa¹, Kaoru Yamaoka¹

5

6 ¹ Department of Rehabilitation, Faculty of Rehabilitation, Hiroshima International
7 University, Kurose-Gakuendai 555-36, Higashi-Hiroshima, Hiroshima, Japan

8

9 Corresponding author

10 Junya Ozawa

11 Department of Rehabilitation, Faculty of Rehabilitation, Hiroshima International

12 University, Kurose-Gakuendai 555-36, Higashi-Hiroshima, Hiroshima, 739-2695, Japan

13 E-mail: j-ozawa@hirokoku-u.ac.jp

14 Tel: +81-823-70-4547

15 Fax: +81-823-70-4542

16

17 Short title: MMC prevents remobilization-induced arthrogenic contracture

18

19

20

21 **Summary**

22 This study tested whether cell cycle inhibitor mitomycin C (MMC) prevents arthrogenic
23 contracture progression during remobilization by inhibiting fibroblast proliferation and
24 fibrosis in the joint capsule. Rat knees were immobilized in a flexed position to generate
25 flexion contracture. After three weeks, the fixation device was removed and rat knees
26 were allowed to freely move for one week. Immediately after and three days after fixator
27 removal, rats received intra-articular injections of MMC or saline. The passive extension
28 range of motion (ROM) was measured before and after myotomy of the knee flexors to
29 distinguish myogenic and arthrogenic contractures. In addition, both cellularity and
30 fibrosis in the posterior joint capsule were assessed histologically. Joint immobilization
31 significantly decreased ROMs both before and after myotomy compared with untreated
32 controls. In saline-injected knees, remobilization increased ROM before myotomy, but
33 further decreased that after myotomy compared with that of knees immediately after three
34 weeks of immobilization. Histological analysis revealed that hypercellularity, mainly due
35 to fibroblast proliferation, and fibrosis characterized by increases in collagen density and
36 joint capsule thickness occurred after remobilization in saline-injected knees. Conversely,
37 MMC injections were able to prevent the remobilization-enhanced reduction of ROM
38 after myotomy by inhibiting both hypercellularity and joint capsule fibrosis. Our results

39 suggest that joint capsule fibrosis accompanied by fibroblast proliferation is a potential
40 cause of arthrogenic contracture progression during remobilization, and that inhibiting
41 fibroblast proliferation may constitute an effective remedy.

42

43 Key words: Joint contracture, Immobilization, Fibroblast, Fibrosis, Mitomycin C

44

45 **Introduction**

46 Joint immobilization is frequently used to treat orthopedic disorders such as bone
47 fractures and ligamentous injuries, but often causes joint contracture (Chesworth and
48 Vandervoort 1995, Moseley *et al.* 2005, Nightingale *et al.* 2007), which is characterized
49 by a reduced passive range of motion (ROM) of the joint (Wong *et al.* 2015). As joint
50 contractures can lead to various types of locomotive disabilities (Bot *et al.* 2012, De Smet
51 2007), management of this impairment is a critical issue in the field of orthopedics.

52 Because joint immobilization is a major cause of joint contracture, it is clinically
53 accepted that joint movement during remobilization is effective in improving joint
54 contracture. Passive joint movements such as stretching are frequently applied in this
55 context. In animal studies, however, it remains controversial whether stretching has
56 beneficial effects on immobilization-induced joint contracture (Kondo *et al.* 2012, Okita
57 *et al.* 2001, Usuba *et al.* 2007). In humans, a clinical study failed to show related benefits
58 of passive stretching (Moseley *et al.* 2005), and recent reviews supported by high-quality
59 evidence suggest that stretching does not have a clinically important role in joint
60 contracture treatment (Harvey *et al.* 2017a, Harvey *et al.* 2017b). More reasonable and
61 effective treatment approaches are therefore needed.

62 Formation and recovery processes of immobilization-induced joint contracture

63 have been closely examined using animal models. The responsible structures have been
64 broadly divided into myogenic and arthrogenic factors (Nagai *et al.* 2014, Trudel and
65 Uthoff 2000, Trudel *et al.* 2014). Trudel et al. demonstrated that a myogenic factor is
66 mainly responsible for joint contracture in the early phases of immobilization (within two
67 weeks) and is resolved by remobilization (Trudel *et al.* 2014). In contrast, arthrogenic
68 factors largely contribute to severe joint contracture induced by prolonged (over four
69 weeks) immobilization, and recovery by remobilization is not expected in these cases
70 (Trudel *et al.* 2014). Arthrogenic contracture also further progresses during
71 remobilization following short-term (within three weeks) immobilization (Kaneguchi and
72 Ozawa 2017, Kaneguchi *et al.* 2017, Kaneguchi *et al.* 2018a, Kaneguchi *et al.* 2018b,
73 Kaneguchi *et al.* 2019, Trudel *et al.* 2014). To avoid irreversible joint contracture,
74 arthrogenic contracture should therefore be targeted.

75 Fibrosis in the joint components is believed to be the major factor contributing
76 to development of arthrogenic contracture in injured (Fukui *et al.* 2000, Fukui *et al.* 2001,
77 Gao *et al.* 2017, Li *et al.* 2013a) and immobilized joints (Sasabe *et al.* 2017). For example,
78 administration of decorin, which suppresses bioactivity of cell adhesion, as well as
79 fibrotic regulators, such as transforming growth factor-beta, can improve restricted joint
80 motion in the rabbit intra-articular adhesion model (Fukui *et al.* 2001). However, several

81 studies showed development of arthrogenic contracture without fibrosis in the
82 periarticular connective tissue in spinal cord injury and immobilization models (Hagiwara
83 *et al.* 2010, Kaneguchi *et al.* 2017, Kaneguchi *et al.* 2018a, Kaneguchi *et al.* 2018b,
84 Kaneguchi *et al.* 2019, Moriyama *et al.* 2007). While it therefore remains controversial
85 whether joint fibrosis is a major factor in arthrogenic contracture, development of fibrosis
86 is observed in the joint capsule of remobilized joints together with progression of
87 arthrogenic contracture (Kaneguchi *et al.* 2017, Kaneguchi *et al.* 2018a, Kaneguchi *et al.*
88 2018b, Kaneguchi *et al.* 2019). We previously showed that anti-inflammatory treatment
89 using the steroidal drug dexamethasone can prevent remobilization-induced arthrogenic
90 contracture progression by suppressing joint capsule fibrosis and fibroblast proliferation
91 (Kaneguchi *et al.* 2018b). Other studies using intra-articular adhesion models also
92 reported that administration of anti-inflammatory agents such as celecoxib and botulinum
93 toxin type A attenuates joint contracture and intra-articular adhesion as well as fibroblast
94 proliferation (Baranowski *et al.* 2019, Gao *et al.* 2017, Li *et al.* 2013a). Fibroblasts
95 produce extracellular matrix proteins such as collagens, and thus fibroblast proliferation
96 is an important process in the development of joint fibrosis (Emami *et al.* 2012, Li *et al.*
97 2014). We therefore suggest that proliferation of fibroblasts triggered by inflammation
98 plays an important role in forming joint capsule fibrosis and that inhibition of fibrosis

99 may be essential for blocking the progression of arthrogenic contracture.

100 To inhibit fibroblast proliferation, we focused on the cell cycle inhibitor
101 mitomycin C (MMC). In a clinical context, MMC is generally used as an anti-cancer drug
102 (Kahmann *et al.* 2010). However, it also finds application pre-clinically and clinically as
103 an anti-fibrotic drug for keloid, capsular contracture, and scarring after ocular surgery
104 (Lane *et al.* 2003, Li *et al.* 2013b, Nava *et al.* 2017, Sidle and Kim 2011, Simman *et al.*
105 2003, Wang *et al.* 2012). MMC can attenuate the development of fibrosis as well as inhibit
106 fibroblast proliferation in injury-induced intra-articular adhesion models (Kocaoglu *et al.*
107 2011, Li *et al.* 2013b, Wang *et al.* 2012).

108 Therefore, we hypothesized that remobilization-induced joint capsule fibrosis
109 and progression of arthrogenic contracture would also be attenuated by MMC
110 administration via inhibition of fibroblast proliferation. To test this hypothesis, we
111 investigated the effects of MMC on joint ROM and histopathology in the remobilized rat
112 knee.

113

114 **Materials and methods**

115 *Experimental animals*

116 Twenty-five eight-week-old male Wistar rats (190–220 g; Japan SLC, Shizuoka, Japan)

117 were used in this study. The rats were randomly divided into four groups: control (n = 4),
118 immobilization (IM: n = 7), remobilization with saline injections after immobilization
119 (RM: n = 7), and remobilization with MMC injections after immobilization (RM + M: n
120 = 7). In the control group, data from the right and left knees were treated as individual
121 samples; therefore, we used data of eight knees from four rats as control. Rats were
122 housed in standard cages in a temperature-controlled room (20°C–25°C) with 12 h
123 light/dark cycles. Standard rodent chow and water were provided *ad libitum*. This
124 experimental design was approved by the committee on animal experimentation of
125 Hiroshima International University.

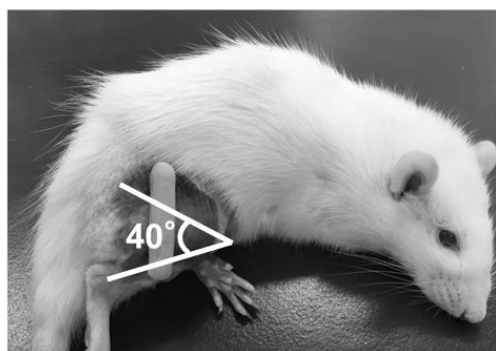
126

127 *Joint immobilization and remobilization*

128 The right knees of rats in the IM, RM, and RM + M groups were immobilized with an
129 external fixator according to the method described in previous studies (Nagai *et al.* 2014,
130 Ozawa *et al.* 2016). In brief, after anesthesia by intraperitoneal injection of sodium
131 pentobarbital (32.4 mg/kg of body weight), Kirschner wires (01-132-50; MIZUHO,
132 Tokyo, Japan) were screwed into the femur and the tibia and were fixed by wire and resin
133 (Provinice Fast; Matsukaze, Kyoto, Japan) to immobilize knee joints at a flexion of
134 approximately 140° (Fig. 1). During immobilization, rats could move freely using their

135 four limbs. Knees in the control group were untreated. After three weeks, the fixation
136 device was removed and rats in the RM and RM + M groups were allowed to recover for
137 one week (remobilization). It is known that one week of remobilization following three
138 weeks of immobilization induces fibrotic reactions in the joint capsule and arthrogenic
139 contracture progression (Kaneguchi *et al.* 2017, Kaneguchi *et al.* 2018a, Kaneguchi *et al.*
140 2018b, Kaneguchi *et al.* 2019). Rats in the IM group were analyzed immediately after
141 removal of the fixator and represented data from immobilization without remobilization.
142 Therefore, data in the control and IM groups were collected at three weeks after starting
143 the experiment, while data in the RM and RM + M groups were collected at four weeks.
144

Fig. 1



145
146 Figure 1: Image of joint immobilization. The right knee joint is immobilized at a flexion
147 of approximately 140° (angle between the femur and the fibula is 40°) by an
148 external fixator.

149

150 *MMC treatment*

151 To inhibit remobilization-induced fibroblast proliferation, rats in the RM + M group
152 received intra-articular injections of 0.08 mg of MMC (concentration 0.8 mg/mL).
153 Because cell proliferation is active until three days after fixator removal (Kaneguchi *et al.*
154 2017), injections were given immediately after and three days after removal. The quantity
155 of MMC administered was determined based on the literature to achieve an anti-
156 proliferative effect (Kocaoglu *et al.* 2011). In the RM group, rats received intra-articular
157 injections of the same volume of saline (0.1 mL) at the same time. Thus, rats in the RM
158 and RM + M groups received two injections.

159

160 *ROM measurements*

161 At the end of experimental periods, we measured ROMs according to the method of our
162 previous study (Kaneguchi *et al.* 2015). In brief, rats were anesthetized with
163 intraperitoneal injection of sodium pentobarbital (32.4 mg/kg of body weight). After rat
164 hindlimbs were skinned, rats were placed in the neutral spine position and the femur was
165 manually fixed at 90° of the hip flexion, followed by 14.6 N mm of knee extension
166 moment. This moment stretched the knee joint close to its physiological limit (Moriyama

167 *et al.* 2006), but did not disrupt the knee soft tissues (Trudel and Uthoff 2000). Using a
168 3D motion analysis system (Kinema Tracer; Kissei Comtec, Nagano, Japan), the angle
169 between the femur and fibula was measured as ROM before myotomy. Then, rats were
170 sacrificed by exsanguination under sodium pentobarbital anesthesia, and knee flexor
171 muscles were completely transected to remove the myogenic factor. Finally, ROM after
172 myotomy was measured to evaluate arthrogenic contracture.

173

174 *Histological assessment*

175 Tissue preparation

176 After ROM measurements, the knee joints were harvested and immersion-fixed at flexion
177 90° in 0.1 M phosphate-buffered 4% paraformaldehyde (pH 7.4) for 48 hours at 4°C.
178 After fixation, samples were decalcified by 17.7% ethylenediaminetetraacetic acid (pH
179 7.2, Osteosoft; Merck Millipore, Darmstadt, Germany) and embedded in paraffin. Using
180 a microtome, samples were cut into 4 µm sagittal sections at the medial mid condylar
181 level.

182

183 Cell counting

184 Counting of cells was performed according to the methods described in previous studies

185 (Kaneguchi *et al.* 2017, Kaneguchi *et al.* 2018a). In brief, sections were stained with
186 hematoxylin and eosin. We photographed the superior, central, and inferior regions of the
187 posterior joint capsule at 40× magnification and manually counted the number of cells.
188 Cell numbers were then converted to cells per mm² of joint capsule.

189

190 Counting of fibroblasts

191 To visualize fibroblasts, we performed immunohistochemistry using anti-vimentin
192 antibodies. Deparaffinized sections were treated with 1% trypsin for 5 min at 37°C for
193 antigen retrieval. To quench endogenous peroxidase activity, sections were incubated
194 with methanol containing 3% H₂O₂ for 30 min. Nonspecific binding was blocked by 1%
195 normal horse serum in 0.01 M phosphate-buffered saline (PBS; pH 7.4) for 30 min. We
196 then incubated sections with anti-vimentin antibody (1:1000 dilution; ab92547, Abcam,
197 Cambridge, UK) for three hours at room temperature followed by rinsing with PBS.
198 Secondary antibody (horse biotinylated anti-mouse/rabbit IgG, 1:250 dilution; BA-1400,
199 Vector Laboratories, Burlingame, CA, USA) was added for 30 min. After rinsing with
200 PBS, we incubated sections with a streptavidin-biotin complex (1:50 dilution; Elite ABC,
201 Vector Laboratories) for 30 min. Finally, immunoreactivity was visualized with a Dako
202 EnVision+ kit/HRP (DAB) (Dako Japan, Tokyo, Japan), followed by counterstaining with

203 hematoxylin. While vimentin is often used as a fibroblast marker (Abdul *et al.* 2015,
204 Glazebrook *et al.* 2008, Krejci *et al.* 2015, Wang *et al.* 2014), it is also expressed in other
205 cell types, including endothelial cells, macrophages, neutrophils, and lymphocytes (Evans
206 1998). Therefore, spindle-shaped vimentin-positive cells not detected in luminal
207 structures were considered fibroblasts (Kaneguchi *et al.* 2018a). Counting of fibroblasts
208 was performed in the same way as cell counting.

209

210 Calculating joint capsule collagen density

211 We calculated collagen density following methods described previously (Kaneguchi *et al.*
212 2017). In brief, sections were stained with aldehyde fuchsin-Masson Goldner (AFMG) to
213 identify collagen. We captured the posterior joint capsule just behind the meniscus at 20×
214 magnification (Fig. 2A and B) and analyzed the digitized image using ImageJ software
215 (National Institutes of Health, Bethesda, MD, USA). To isolate collagen, we extracted
216 green color from the original color image using the Split Channels function. Using the
217 Threshold function, an arbitrary threshold was set to determine the green stained area.
218 Collagen density was calculated by dividing this area by the total joint capsule area.

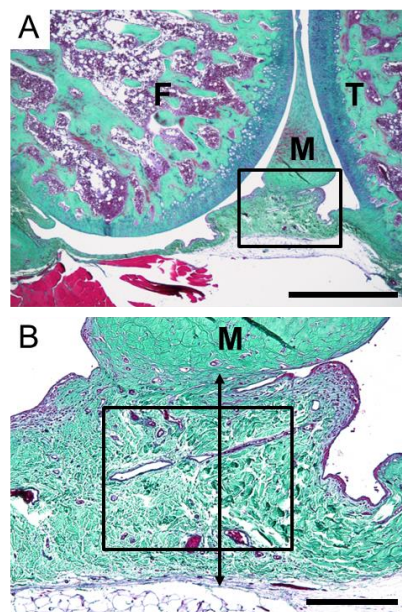
219

220 Measurement of joint capsule thickness.

221 Using AFMG-stained sections, the thickness of the posterior joint capsule was measured
222 according to the methods described previously (Kaneguchi *et al.* 2017). In brief, after the
223 posterior region of the knee joint was photographed at 2× magnification, the distance
224 between the posterior borders of the meniscus and the joint capsule was measured as joint
225 capsule thickness using ImageJ software (Fig. 2A and B). All analyses were performed in
226 an unblinded manner.

227

Fig. 2



228

229 Figure 2: Images of morphometrical and histological analyses of the posterior joint
230 capsule. A shows example image of the posterior knee joint stained with aldehyde
231 fuchsin-Masson Goldner. High magnification of the box in A is shown in B. The
232 distance between the posterior borders of the meniscus and the joint capsule (up-

233 down arrow) was measured as posterior joint capsule thickness (B). In addition,
234 collagen density (percentage of green stained area) was also measured in the
235 posterior joint capsule (box in B). F, femur; T, tibia; M, meniscus. Scale bars = 1
236 mm in A, 200 μ m in B.

237

238

239 *Statistical analysis*

240 We performed statistical analyses using Dr. SPSS II for Windows (SPSS Japan Inc.,
241 Tokyo, Japan) and G*Power 3.1 (University of Düsseldorf, Düsseldorf, Germany).
242 Normality of the distribution and homogeneity of variance were tested using the
243 Kolmogorov-Smirnov and Levene tests, respectively. All data met normality and
244 homoscedasticity assumptions. Therefore, one-way analysis of variance (ANOVA) and
245 the Tukey's post-hoc test were applied. For all tests, a P-value of < 0.05 was considered
246 statistically significant. A post hoc power analysis was performed using G*Power 3.1.

247

248 **Results**

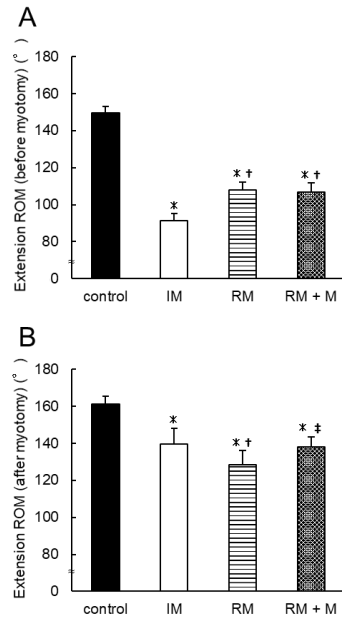
249 *ROM*

250 Knee extension ROMs before myotomy were $149 \pm 4^\circ$, $91 \pm 4^\circ$, $108 \pm 4^\circ$, and $107 \pm 5^\circ$

251 in the control, IM, RM, and RM + M groups, respectively (Fig. 3A). Compared with the
252 control group, ROMs were significantly reduced in all joint-immobilized groups ($P <$
253 0.001). Among immobilized groups, ROMs in the RM and RM + M groups were
254 significantly larger than that in the IM group ($P < 0.001$). Between the RM and RM + M
255 groups, there was no difference in ROM before myotomy ($P = 0.952$). The statistical
256 power for ROM before myotomy was 1.00.

257 Knee extension ROMs after myotomy, which can indicate restriction of ROM
258 caused by arthrogenic factor, were $161 \pm 4^\circ$, $139 \pm 8^\circ$, $128 \pm 8^\circ$, and $138 \pm 5^\circ$ in the
259 control, IM, RM, and RM + M groups, respectively (Fig. 3B). In all joint-immobilized
260 groups, ROMs were significantly reduced compared with the control group ($P < 0.001$).
261 Among immobilized groups, ROM in the RM group was significantly lower than in the
262 IM group ($P = 0.019$). However, ROM in the RM + M group did not differ from the IM
263 group ($P = 0.977$), but was significantly larger than in the RM group ($P = 0.048$). The
264 statistical power for ROM after myotomy was 1.00.

Fig. 3



265

266 Figure 3: Changes in knee extension ROM before and after myotomy. A shows ROM

267 before myotomy. In the IM group, ROM before myotomy was significantly smaller than

268 that in the control group. In the RM and RM + M groups, ROM before myotomy partially

269 recovered, but was still significantly smaller than that in the control group. There was no

270 difference in ROM before myotomy between the RM and RM + M groups. B shows ROM

271 after myotomy. In the IM group, ROM after myotomy was also significantly smaller than

272 that in the control group. In the RM group, ROM after myotomy further decreased

273 compared with the IM group. In the RM + M group, we prevented remobilization-induced

274 progression of ROM restriction. Values are mean + standard deviation. *: indicates

275 significant difference compared with the control group ($P < 0.05$). †: indicates significant

276 difference compared with the IM group ($P < 0.05$). ‡: indicates significant difference

277 compared with the RM group ($P < 0.05$).

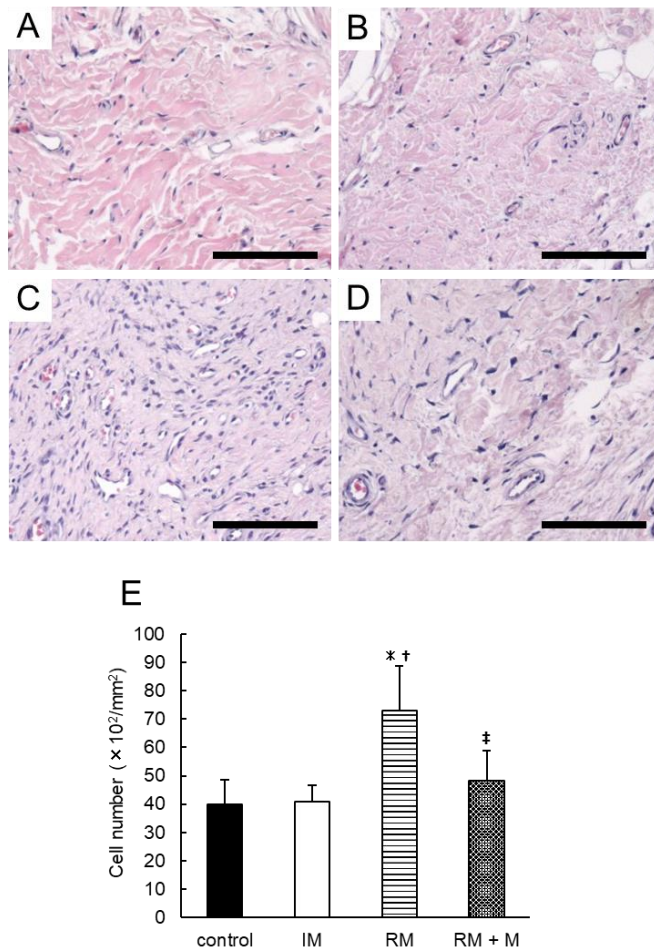
278

279 *Cellularity*

280 In the posterior joint capsule of the control (Fig. 4A) and IM (Fig. 4B) groups, we mainly
281 observed spindle-shaped fibroblast-like cells and vascular endothelial cells, concluding
282 there was no difference in cell number between these two groups ($P = 0.998$, $3,985 \pm 867$
283 and $4,084 \pm 569$ cells/mm², respectively, Fig. 4E). Compared with the control and IM
284 groups, we observed a greater cell number mainly due to proliferated spindle-shaped
285 fibroblast-like cells in the RM group ($P < 0.001$, $7,291 \pm 1,572$ cells/mm², 183% of the
286 control group, Fig. 4C). In the RM + M group (Fig. 4D), cell number was significantly
287 smaller than in the RM group ($P = 0.001$, $4,833 \pm 1,044$ cells/mm², 66% of RM group),
288 but not significantly different from the control and IM groups ($P = 0.468$ and 0.570 ,
289 respectively, 121% of the control group). The statistical power for cell number was 0.95.

290

Fig. 4



291

292 Figure 4: Cellularity of posterior joint capsule. A–D shows the posterior knee joint

293 capsule stained with hematoxylin and eosin. (A) control, (B) IM, (C) RM, and (D)

294 RM + M groups. Scale bars = 100 μm . E shows cell number. There was no

295 difference in cell number between the control and IM groups. In the RM group,

296 we observed many spindle-shaped fibroblast-like cells and, consequently, cell

297 number was significantly higher than in the control and IM groups.

298 Remobilization-induced hypercellularity was prevented in the RM + M group.

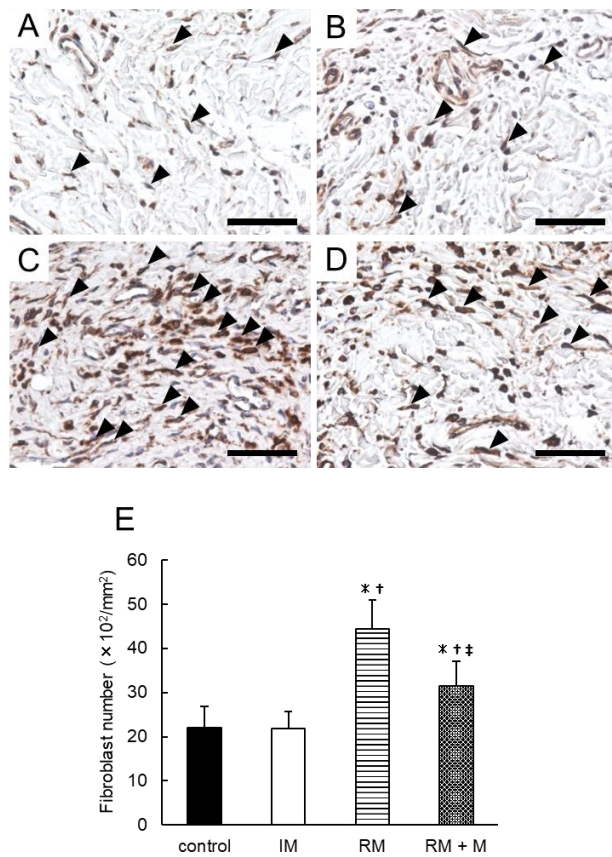
299 Values are mean + standard deviation. *: indicates significant difference compared
300 with the control group ($P < 0.05$). †: indicates significant difference compared
301 with the IM group ($P < 0.05$). ‡: indicates significant difference compared with
302 the RM group ($P < 0.05$).

303

304 The number of vimentin-positive fibroblasts also did not differ between the
305 control (Fig. 5A) and IM (Fig. 5B) groups ($P = 1.000$, $2,199 \pm 491$ and $2,180 \pm 393$
306 cells/mm², respectively, Fig. 5E). Vimentin-positive fibroblast number in the RM group
307 (Fig. 5C) was significantly higher than those in the control and IM groups ($P < 0.001$,
308 $4,434 \pm 660$ cells/mm², 202% of the control group). Also, in the RM + M group (Fig.
309 5D), vimentin-positive fibroblast number was significantly higher than those in the
310 control and IM groups ($P = 0.014$ and 0.012 , respectively, $3,149 \pm 556$ cells/mm², 143%
311 of the control group). However, the number of vimentin-positive fibroblasts was
312 significantly smaller in the RM + M group than in the RM group ($P = 0.001$, 71% of
313 RM group). The statistical power for fibroblast number was 1.00.

314

Fig. 5



315

316 Figure 5: Fibroblast number in the posterior joint capsule. A–D shows posterior knee joint

317 capsule immunohistochemically stained with anti-vimentin antibody. (A) control,

318 (B) IM, (C) RM, and (D) RM + M groups. Arrowheads indicate fibroblasts. Scale

319 bars = 50 μ m. E shows fibroblast number. There was no difference in fibroblast

320 number between the control and IM groups. Compared with those in the control

321 and IM groups, the number of fibroblasts in the RM group increased. In the RM

322 + M group, an increase in fibroblasts was partially attenuated. Values are mean +

323 standard deviation. *: indicates significant difference compared with the control

324 group ($P < 0.05$). †: indicates significant difference compared with the IM group
325 ($P < 0.05$). ‡: indicates significant difference compared with the RM group ($P <$
326 0.05).

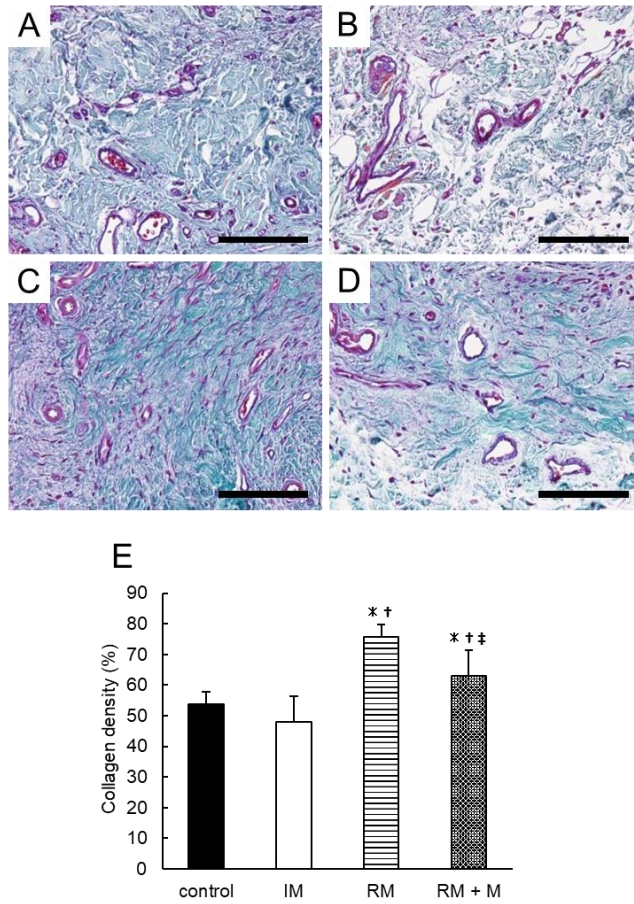
327

328 *Collagen density*

329 In the control (Fig. 6A) and IM (Fig. 6B) groups, collagen fiber bundles in the posterior
330 joint capsule were arranged with gaps. Collagen density was $54 \pm 4\%$ and $48 \pm 8\%$,
331 respectively. There was no significant difference in collagen density between the control
332 and IM groups ($P = 0.324$, Fig. 6E). In the RM group (Fig. 6C), the gap of collagen fiber
333 bundles disappeared and collagen density increased to $76 \pm 4\%$, significantly different to
334 the control and IM groups ($P < 0.001$). In the RM + M group (Fig. 6D), gaps between
335 collagen fiber bundles were partially restored and collagen density was $63 \pm 8\%$. Collagen
336 density in the RM + M group was significantly lower than that in the RM group ($P =$
337 0.006), but significantly higher than in the control and IM groups ($P = 0.043$ and 0.001 ,
338 respectively). The statistical power for collagen density was 1.00.

339

Fig. 6



340

341 Figure 6: Morphological changes in the posterior knee joint capsule. A–D shows posterior

342 knee joint capsule stained with aldehyde fuchsin-Masson Goldner. (A) control,

343 (B) IM, (C) RM, and (D) RM + M groups. Collagen is stained green. Scale bars

344 = 100 μ m. E shows collagen density. There was no difference in collagen density

345 between the control and IM groups. In the RM group, the gaps of collagen bundles

346 narrowed and joint capsules became denser. Consequently, collagen density in the

347 RM group significantly increased compared with the control and IM groups. In

348 the RM + M group, a remobilization-induced increase in collagen density was

349 partially attenuated. Values are mean + standard deviation. *: indicates significant
350 difference compared with the control group ($P < 0.05$). †: indicates significant
351 difference compared with the IM group ($P < 0.05$). ‡: indicates significant
352 difference compared with the RM group ($P < 0.05$).

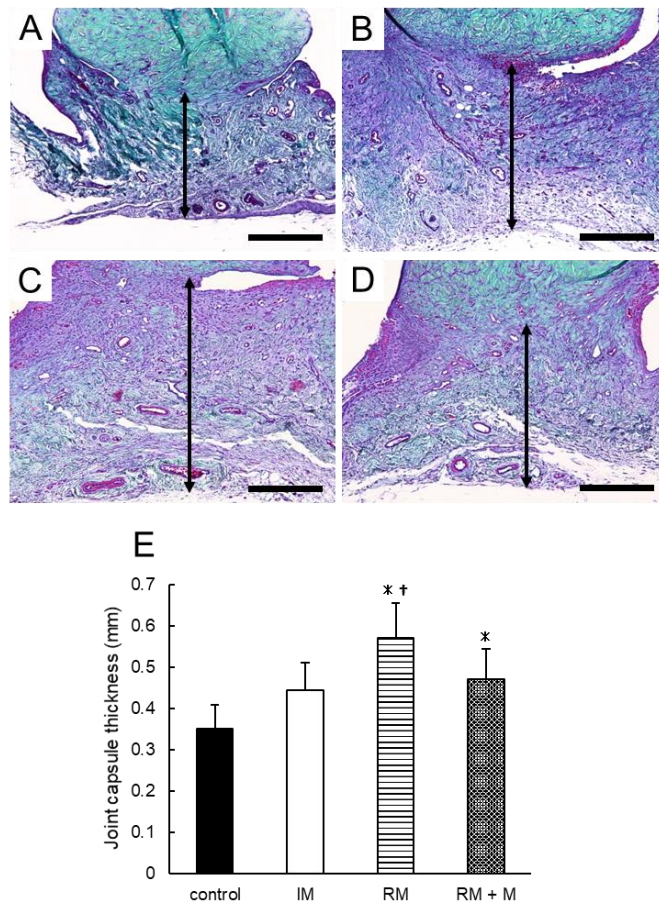
353

354 *Joint capsule thickness*

355 In the control group (Fig. 7A), joint capsule thickness was 0.35 ± 0.06 mm (Fig. 7E). In
356 the IM group (Fig. 7B), the posterior joint capsule was slightly thickened (0.45 ± 0.07
357 mm), but not significantly, compared with that in the control group ($P = 0.077$). Joint
358 capsule thickness in the RM group was 0.57 ± 0.09 mm (Fig. 7C) and was significantly
359 thicker than those in the control and IM groups ($P < 0.001$ and $P = 0.014$, respectively).
360 In the RM + M group (Fig. 7D), joint capsule thickness tended to be lower than in the
361 RM groups (0.47 ± 0.07 mm, $P = 0.067$) and was comparable to the IM group ($P = 0.901$).
362 The statistical power for joint capsule thickness was 0.98.

363

Fig. 7



364

365 Figure 7: Thickness in the posterior joint capsule. A–D shows posterior knee joint capsule

366 stained with aldehyde fuchsin-Masson Goldner. (A) control, (B) IM, (C) RM, and

367 (D) RM + M groups. Up-down arrows indicate posterior joint capsule thickness.

368 Scale bars = 200 μ m. E shows joint capsule thickness. Compared with the control

369 group, the posterior joint capsule in the IM group was slightly thickened, but

370 differences were not significant ($P = 0.077$). Joint capsule thickness in the RM

371 group was significantly larger than those in the control and IM groups. In the RM

372 + M group, joint capsule thickness tended to be smaller than in the RM groups (P

373 = 0.067) and was comparable to the IM group. Values are mean + standard
374 deviation. *: indicates significant difference compared with the control group (P
375 < 0.05). †: indicates significant difference compared with the IM group (P < 0.05).

376

377 **Discussion**

378 In this study, we tested whether MMC administration prevents the progression of
379 remobilization-induced arthrogenic contracture by inhibiting fibroblast proliferation and
380 fibrosis in the joint capsule. As expected, MMC injections served to attenuate progression
381 of arthrogenic contracture by suppressing fibroblast proliferation, leading to significantly
382 lower collagen density and a tendency to be lower joint capsule thickness. These results
383 suggest that joint capsule fibrosis is a potential cause of arthrogenic contracture
384 progression in remobilized joints.

385 Three weeks of immobilization significantly reduced ROMs both before and
386 after myotomy. After one week of remobilization, ROM before myotomy increased but
387 after myotomy further decreased. These results indicate that remobilization improves
388 myogenic contracture, but aggravates arthrogenic contracture oppositely. Although
389 immobilization-induced arthrogenic contracture is not improved by remobilization
390 (Kaneguchi *et al.* 2017, Kaneguchi *et al.* 2018a, Kaneguchi *et al.* 2018b, Kaneguchi *et al.*

391 2019, Trudel *et al.* 2014), arthrogenic contracture in intra-articular adhesion model using
392 joint immobilization with intra-articular injury partially recovers after remobilization
393 (Baranowski *et al.* 2018). These findings suggest that arthrogenic contracture attributed
394 to intra-articular injury may be variable in contrast with immobilization only. Intra-
395 articular injections of MMC during remobilization could prevent further decrease in
396 ROM after myotomy, which may be due to intra-articular (micro) injury (Kaneguchi *et*
397 *al.* 2017). However, MMC injections did not improve ROM before myotomy. Our results
398 indicate that MMC has beneficial effects on arthrogenic contracture but not on myogenic
399 one.

400 Fibrosis in joint components strongly contributes to progressing arthrogenic
401 contracture in remobilized (Kaneguchi *et al.* 2017, Kaneguchi *et al.* 2018a, Kaneguchi *et*
402 *al.* 2018b) as well as injured joints (Fukui *et al.* 2000, Fukui *et al.* 2001, Gao *et al.* 2017,
403 Li *et al.* 2013a). Further, we observed increased joint capsule thickness and collagen
404 density in the joint capsule following remobilization together with progressing
405 arthrogenic contracture. Extracellular matrix proteins, such as collagen, are produced by
406 fibroblasts. In joint injury-induced contracture, inhibiting fibroblast proliferation by anti-
407 proliferative agents MMC or hydroxycamptothecin can attenuate fibrosis in intra-
408 articular adhesion sites (Li *et al.* 2013b, Liang *et al.* 2014). Therefore, it seems likely that

409 fibroblast proliferation plays an important role in generating joint fibrosis. In our present
410 and previous studies, we observed development of joint capsule fibrosis together with
411 fibroblast proliferation during remobilization (Kaneguchi *et al.* 2017, Kaneguchi *et al.*
412 2018a, Kaneguchi *et al.* 2018b, Kaneguchi *et al.* 2019), suggesting that fibroblast
413 proliferation contributes to fibrosis formation in remobilized joints. We previously
414 revealed that administering the steroidal anti-inflammatory drug dexamethasone during
415 remobilization can prevent joint capsule fibrosis by suppressing hypercellularity with
416 increasing fibroblast numbers (Kaneguchi *et al.* 2018b). In the present study,
417 administering MMC, which selectively prevents cell proliferation without inhibiting
418 inflammation, was also able to attenuate joint capsule fibrosis; this prevented arthrogenic
419 contracture progression during remobilization. We previously reported that inflammatory
420 reactions reach their peak within one day of remobilization, but that arthrogenic
421 contracture progression is not observed at that point (Kaneguchi *et al.* 2017). Progression
422 of arthrogenic contracture characterized by development of joint capsule fibrosis is
423 observed only after inflammation (Kaneguchi *et al.* 2017). These findings suggest that
424 fibroblast proliferation (and subsequent upregulation of collagens) triggered by
425 inflammation plays an important role in driving fibrotic processes, which induces
426 arthrogenic contracture progression in remobilized joints.

427 In immobilized joints, remobilization can improve myogenic (Kaneguchi *et al.*
428 2017, Trudel *et al.* 2014) but not arthrogenic contracture (Kaneguchi and Ozawa 2017,
429 Kaneguchi *et al.* 2017, Kaneguchi *et al.* 2018a, Kaneguchi *et al.* 2018b, Kaneguchi *et al.*
430 2019, Trudel *et al.* 2014). Therefore, effective therapeutic interventions for arthrogenic
431 contracture are needed to avoid permanent joint contracture. Some animal and clinical
432 studies reported the effectiveness of anti-inflammatory and anti-fibrotic agents on the
433 attenuation of joint contracture (Baranowski *et al.* 2019, Usher *et al.* 2019). In the clinical
434 setting, however, treatment options for joint contracture are limited to passive joint
435 movements such as stretching, manipulation under anaesthesia (MUA), or surgical
436 treatments (Charalambous and Morrey 2012, Wong *et al.* 2015). Previous studies identify
437 no positive effects of stretching on joint contracture (Harvey *et al.* 2017a, Harvey *et al.*
438 2017b, Moseley *et al.* 2005). MUA and surgical treatments are effective to improve joint
439 contracture, but have the risk of complications, including nerve symptoms, heterotopic
440 ossification, and instability (Cai *et al.* 2015, Usher *et al.* 2019). Developing new
441 therapeutic strategies as alternatives to current treatments is therefore a critical concern
442 (Wong *et al.* 2015). In this study, we demonstrated that intra-articular injections of the
443 cell cycle inhibitor MMC effectively attenuates remobilization-induced joint capsule
444 fibrosis and arthrogenic contracture progression. Inhibiting fibroblast proliferation during

445 remobilization may become a novel therapeutic strategy in treating immobilization-
446 induced arthrogenic contracture.

447 This study has some limitations. First, all analyses were performed in an
448 unblinded manner. We thus cannot exclude the possibility of the subjective bias. Second,
449 we immobilized knee joint using external fixator constructed by Kirschner wires, wire,
450 and resin. Cast immobilization might be more suitable to mimic the human situation after
451 the orthopedic disorders. Third, immunohistochemistry was performed only for the
452 fibroblast. Both fibroblasts and myofibroblasts are major contributors to fibrotic changes
453 (Hinz *et al.* 2012, Kendall and Feghali-Bostwick 2014). In particular, myofibroblasts
454 expressing α -smooth muscle actin (α -SMA) have high extracellular matrix protein
455 production capacity (Hinz *et al.* 2012, Kendall and Feghali-Bostwick 2014) and thus play
456 a central role in joint fibrosis (Baranowski *et al.* 2019, Li *et al.* 2013b). Identification of
457 myofibroblasts by α -SMA would give valuable information.

458 In conclusion, the present study demonstrated that inhibiting fibroblast
459 proliferation by intra-articular MMC injections during remobilization can benefit the
460 treatment of arthrogenic contracture by attenuating joint capsule fibrosis.

461

462 **Conflict of Interest**

463 There is no conflict of interest.

464

465 **Acknowledgements**

466 This study was supported by a grant from the Japanese Physical Therapy Association.

467

468 **References**

469 Abdul N, Dixon D, Walker A, Horabin J, Smith N, Weir DJ, Brewster NT, Deehan DJ,

470 Mann DA, Borthwick LA: Fibrosis is a common outcome following total knee

471 arthroplasty. *Sci Rep* **5**: 16469, 2015.

472 Baranowski A, Schlemmer L, Forster K, Mattyasovszky SG, Ritz U, Wagner D,

473 Rommens PM, Hofmann A: A novel rat model of stable posttraumatic joint

474 stiffness of the knee. *Journal of orthopaedic surgery and research* **13**: 185, 2018.

475 Baranowski A, Schlemmer L, Forster K, Slotina E, Mickan T, Truffel S, Klein A,

476 Mattyasovszky SG, Hofmann A, Ritz U, Rommens PM: Effects of losartan and

477 atorvastatin on the development of early posttraumatic joint stiffness in a rat

478 model. *Drug Des Devel Ther* **13**: 2603-2618, 2019.

479 Bot AG, Souer JS, van Dijk CN, Ring D: Association between individual DASH tasks and

480 restricted wrist flexion and extension after volar plate fixation of a fracture of the

481 distal radius. *Hand (New York, N.Y.)* **7**: 407-412, 2012.

482 Cai J, Wang W, Yan H, Sun Y, Chen W, Chen S, Fan C: Complications of Open Elbow
483 Arthrolysis in Post-Traumatic Elbow Stiffness: A Systematic Review. *PLoS One*
484 **10**: e0138547, 2015.

485 Charalambous CP, Morrey BF: Posttraumatic elbow stiffness. *J Bone Joint Surg Am* **94**:
486 1428-1437, 2012.

487 Chesworth BM, Vandervoort AA: Comparison of passive stiffness variables and range of
488 motion in uninvolved and involved ankle joints of patients following ankle
489 fractures. *Phys Ther* **75**: 253-261, 1995.

490 De Smet L: Does restricted wrist motion influence the disability of the upper limb? *Acta*
491 *orthopaedica Belgica* **73**: 446-450, 2007.

492 Emami MJ, Jaber FM, Azarpira N, Vosoughi AR, Tanideh N: Prevention of arthrofibrosis
493 by monoclonal antibody against vascular endothelial growth factor: a novel use
494 of bevacizumab in rabbits. *Orthop Traumatol Surg Res* **98**: 759-764, 2012.

495 Evans RM: Vimentin: the conundrum of the intermediate filament gene family. *Bioessays*
496 **20**: 79-86, 1998.

497 Fukui N, Tashiro T, Hiraoka H, Oda H, Nakamura K: Adhesion formation can be reduced
498 by the suppression of transforming growth factor-beta1 activity. *Journal of*

499 *orthopaedic research : official publication of the Orthopaedic Research Society*
500 **18**: 212-219, 2000.

501 Fukui N, Fukuda A, Kojima K, Nakajima K, Oda H, Nakamura K: Suppression of fibrous
502 adhesion by proteoglycan decorin. *Journal of orthopaedic research : official*
503 *publication of the Orthopaedic Research Society* **19**: 456-462, 2001.

504 Gao ZY, Wu JX, Liu WB, Sun JK: Reduction of adhesion formation after knee surgery in
505 a rat model by botulinum toxin A. *Biosci Rep* **37**, 2017.

506 Glazebrook MA, Wright JR, Jr., Langman M, Stanish WD, Lee JM: Histological analysis
507 of achilles tendons in an overuse rat model. *Journal of orthopaedic research :*
508 *official publication of the Orthopaedic Research Society* **26**: 840-846, 2008.

509 Hagiwara Y, Ando A, Onoda Y, Matsui H, Chimoto E, Suda H, Itoi E: Expression patterns
510 of collagen types I and III in the capsule of a rat knee contracture model. *Journal*
511 *of orthopaedic research : official publication of the Orthopaedic Research Society*
512 **28**: 315-321, 2010.

513 Harvey LA, Katalinic OM, Herbert RD, Moseley AM, Lannin NA, Schurr K: Stretch for
514 the treatment and prevention of contractures. *Cochrane Database Syst Rev* **1**:
515 CD007455, 2017a.

516 Harvey LA, Katalinic OM, Herbert RD, Moseley AM, Lannin NA, Schurr K: Stretch for

517 the treatment and prevention of contracture: an abridged republication of a
518 Cochrane Systematic Review. *J Physiother* **63**: 67-75, 2017b.

519 Hinz B, Phan SH, Thannickal VJ, Prunotto M, Desmouliere A, Varga J, De Wever O,
520 Mareel M, Gabbiani G: Recent developments in myofibroblast biology: paradigms
521 for connective tissue remodeling. *The American journal of pathology* **180**: 1340-
522 1355, 2012.

523 Kahmann L, Beyer U, Mehlhorn G, Thiel FC, Strnad V, Fasching PA, Lux MP: Mitomycin
524 C in patients with gynecological malignancies. *Onkologie* **33**: 547-557, 2010.

525 Kaneguchi A, Ozawa J, Moriyama H, Yamaoka K: Structures responsible for the
526 formation of knee joint contracture secondary to adjuvant-induced arthritis in a
527 rat model. *Iryo Kogaku Zasshi (J Med Eng)*: 1-12, 2015.

528 Kaneguchi A, Ozawa J: The preventive effects of low-level laser therapy on arthrogenic
529 contracture progression in remobilized rat knee (in Japanese). *Japanese Journal*
530 *of Electrophysical Agents* **24**: 47-51, 2017.

531 Kaneguchi A, Ozawa J, Kawamata S, Yamaoka K: Development of arthrogenic joint
532 contracture as a result of pathological changes in remobilized rat knees. *Journal*
533 *of orthopaedic research : official publication of the Orthopaedic Research Society*
534 **35**: 1414-1423, 2017.

535 Kaneguchi A, Ozawa J, Minamimoto K, Yamaoka K: Active exercise on immobilization-
536 induced contractured rat knees develops arthrogenic joint contracture with
537 pathological changes. *Journal of applied physiology (Bethesda, Md. : 1985)* **124**:
538 291-301, 2018a.

539 Kaneguchi A, Ozawa J, Yamaoka K: Anti-inflammatory Drug Dexamethasone Treatment
540 During the Remobilization Period Improves Range of Motion in a Rat Knee
541 Model of Joint Contracture. *Inflammation* **41**: 1409-1423, 2018b.

542 Kaneguchi A, Ozawa J, Minamimoto K, Yamaoka K: Low-Level Laser Therapy Prevents
543 Treadmill Exercise-Induced Progression of Arthrogenic Joint Contracture Via
544 Attenuation of Inflammation and Fibrosis in Remobilized Rat Knees.
545 *Inflammation* **42**: 857-873, 2019.

546 Kendall RT, Feghali-Bostwick CA: Fibroblasts in fibrosis: novel roles and mediators.
547 *Front Pharmacol* **5**: 123, 2014.

548 Kocaoglu B, Akgun U, Nalbantoglu U, Poyanli O, Karahan M: Adhesion reduction after
549 knee surgery in a rat model by mitomycin C. *Knee Surg Sports Traumatol Arthrosc*
550 **19**: 94-98, 2011.

551 Kondo Y, Nakano J, Sakamoto J, Kataoka H, Yokoyama S, Honda Y, Origuchi T,
552 Yoshimura T, Okita M: Effects of Prolonged Stretching and Thermotherapy on

553 Muscle Contracture of Immobilized Rat Soleus Muscle. *Journal of Physical*
554 *Therapy Science* **24**: 541-547, 2012.

555 Krejci E, Kodet O, Szabo P, Borsky J, Smetana K, Jr., Grim M, Dvorankova B: In vitro
556 differences of neonatal and later postnatal keratinocytes and dermal fibroblasts.
557 *Physiol Res* **64**: 561-569, 2015.

558 Lane HA, Swale JA, Majmudar PA: Prophylactic use of mitomycin-C in the management
559 of a buttonholed LASIK flap. *J Cataract Refract Surg* **29**: 390-392, 2003.

560 Li F, He B, Liu S, Fan C: Celecoxib effectively inhibits the formation of joint adhesions.
561 *Exp Ther Med* **6**: 1507-1511, 2013a.

562 Li F, Liu S, Fan C: Lentivirus-mediated ERK2 siRNA reduces joint capsule fibrosis in a
563 rat model of post-traumatic joint contracture. *Int J Mol Sci* **14**: 20833-20844,
564 2013b.

565 Li Y, Ma X, Yu P, Wang S: Intra-articular adhesion reduction after knee surgery in rabbits
566 by calcium channel blockers. *Med Sci Monit* **20**: 2466-2471, 2014.

567 Liang Y, Sun Y, Li X, Yan L, Wang J, Hu J, Yu H, Xiao H, Chen H, Sun Z, Cai J, Feng X,
568 Xiong C, He J: The optimal concentration of topical hydroxycamptothecin in
569 preventing intraarticular scar adhesion. *Sci Rep* **4**: 4621, 2014.

570 Moriyama H, Yoshimura O, Sunahori H, Tobimatsu Y: Comparison of muscular and

571 articular factors in the progression of contractures after spinal cord injury in rats.
572 *Spinal Cord* **44**: 174-181, 2006.

573 Moriyama H, Yoshimura O, Kawamata S, Takemoto H, Saka Y, Tobimatsu Y: Alteration
574 of knee joint connective tissues during contracture formation in spastic rats after
575 an experimentally induced spinal cord injury. *Connect Tissue Res* **48**: 180-187,
576 2007.

577 Moseley AM, Herbert RD, Nightingale EJ, Taylor DA, Evans TM, Robertson GJ, Gupta
578 SK, Penn J: Passive stretching does not enhance outcomes in patients with
579 plantarflexion contracture after cast immobilization for ankle fracture: a
580 randomized controlled trial. *Arch Phys Med Rehabil* **86**: 1118-1126, 2005.

581 Nagai M, Aoyama T, Ito A, Iijima H, Yamaguchi S, Tajino J, Zhang X, Akiyama H, Kuroki
582 H: Contributions of biarticular myogenic components to the limitation of the
583 range of motion after immobilization of rat knee joint. *BMC Musculoskelet Disord*
584 **15**: 224, 2014.

585 Nava MB, Rocco N, Catanuto G, Frangou J, Rispoli C, Ottolenghi J, Bruno N, Spano A:
586 Role of Mitomycin C in Preventing Capsular Contracture in Implant-Based
587 Reconstructive Breast Surgery: A Randomized Controlled Trial. *Plast Reconstr*
588 *Surg* **139**: 819-826, 2017.

589 Nightingale EJ, Moseley AM, Herbert RD: Passive dorsiflexion flexibility after cast
590 immobilization for ankle fracture. *Clin Orthop Relat Res* **456**: 65-69, 2007.

591 Okita M, Yoshimura T, Nakano J, Saeki A, Uehara A, Mineshita A, Eguchi K: Effects of
592 Short Duration Stretching on Disuse Muscle Atrophy in Immobilized Rat Soleus
593 Muscles. *J Jpn Phys Ther Assoc* **4**: 1-5, 2001.

594 Ozawa J, Kaneguchi A, Tanaka R, Kito N, Moriyama H: Cyclooxygenase-2 inhibitor
595 celecoxib attenuates joint contracture following immobilization in rat knees. *BMC*
596 *Musculoskelet Disord* **17**: 446, 2016.

597 Sasabe R, Sakamoto J, Goto K, Honda Y, Kataoka H, Nakano J, Origuchi T, Endo D, Koji
598 T, Okita M: Effects of joint immobilization on changes in myofibroblasts and
599 collagen in the rat knee contracture model. *J Orthop Res* **35**: 1998-2006, 2017.

600 Sidle DM, Kim H: Keloids: prevention and management. *Facial Plast Surg Clin North*
601 *Am* **19**: 505-515, 2011.

602 Simman R, Alani H, Williams F: Effect of mitomycin C on keloid fibroblasts: an in vitro
603 study. *Ann Plast Surg* **50**: 71-76, 2003.

604 Trudel G, Uthoff HK: Contractures secondary to immobility: is the restriction articular
605 or muscular? An experimental longitudinal study in the rat knee. *Arch Phys Med*
606 *Rehabil* **81**: 6-13, 2000.

607 Trudel G, Laneuville O, Coletta E, Goudreau L,Uthhoff HK: Quantitative and temporal
608 differential recovery of articular and muscular limitations of knee joint
609 contractures; results in a rat model. *Journal of applied physiology (Bethesda,*
610 *Md. : 1985)* **117**: 730-737, 2014.

611 Usher KM, Zhu S, Mavropalias G, Carrino JA, Zhao J,Xu J: Pathological mechanisms
612 and therapeutic outlooks for arthrofibrosis. *Bone research* **7**: 9, 2019.

613 Usuba M, Akai M, Shirasaki Y,Miyakawa S: Experimental joint contracture correction
614 with low torque--long duration repeated stretching. *Clin Orthop Relat Res* **456**:
615 70-78, 2007.

616 Wang J, Yan L, Sun Y, Wang D, Dai S, Yu T, Gu J, Jiang B, Feng X, Hu H, Wang Q, Yin
617 B,Lv G: A comparative study of the preventive effects of mitomycin C and
618 chitosan on intraarticular adhesion after knee surgery in rabbits. *Cell Biochem*
619 *Biophys* **62**: 101-105, 2012.

620 Wang Z, Wang Y, Xie P, Liu W,Zhang S: Calcium channel blockers in reduction of
621 epidural fibrosis and dural adhesions in laminectomy rats. *Eur J Orthop Surg*
622 *Traumatol* **24 Suppl 1**: S293-298, 2014.

623 Wong K, Trudel G,Laneuville O: Noninflammatory Joint Contractures Arising from
624 Immobility: Animal Models to Future Treatments. *Biomed Res Int* **2015**: 848290,

625 2015.

626

627

628

629 **Figure legends**

630 Figure 1: Image of joint immobilization. The right knee joint is immobilized at a flexion
631 of approximately 140° (angle between the femur and the fibula is 40°) by an
632 external fixator.

633

634 Figure 2: Images of morphometrical and histological analyses of the posterior joint
635 capsule. A shows example image of the posterior knee joint stained with aldehyde
636 fuchsin-Masson Goldner. High magnification of the box in A is shown in B. The
637 distance between the posterior borders of the meniscus and the joint capsule (up-
638 down arrow) was measured as posterior joint capsule thickness (B). In addition,
639 collagen density (percentage of green stained area) was also measured in the
640 posterior joint capsule (box in B). F, femur; T, tibia; M, meniscus. Scale bars = 1
641 mm in A, 200 μm in B.

642

643 Figure 3: Changes in knee extension ROM before and after myotomy. A shows ROM
644 before myotomy. In the IM group, ROM before myotomy was significantly
645 smaller than that in the control group. In the RM and RM + M groups, ROM
646 before myotomy partially recovered, but was still significantly smaller than that
647 in the control group. There was no difference in ROM before myotomy between

648 the RM and RM + M groups. B shows ROM after myotomy. In the IM group,
649 ROM after myotomy was also significantly smaller than that in the control group.
650 In the RM group, ROM after myotomy further decreased compared with the IM
651 group. In the RM + M group, we prevented remobilization-induced progression
652 of ROM restriction. Values are mean + standard deviation. *: indicates significant
653 difference compared with the control group ($P < 0.05$). †: indicates significant
654 difference compared with the IM group ($P < 0.05$). ‡: indicates significant
655 difference compared with the RM group ($P < 0.05$).

656

657 Figure 4: Cellularity of posterior joint capsule. A–D shows the posterior knee joint
658 capsule stained with hematoxylin and eosin. (A) control, (B) IM, (C) RM, and (D)
659 RM + M groups. Scale bars = 100 μm . E shows cell number. There was no
660 difference in cell number between the control and IM groups. In the RM group,
661 we observed many spindle-shaped fibroblast-like cells and, consequently, cell
662 number was significantly higher than in the control and IM groups.
663 Remobilization-induced hypercellularity was prevented in the RM + M group.
664 Values are mean + standard deviation. *: indicates significant difference compared
665 with the control group ($P < 0.05$). †: indicates significant difference compared

666 with the IM group ($P < 0.05$). ‡: indicates significant difference compared with
667 the RM group ($P < 0.05$).

668

669 Figure 5: Fibroblast number in the posterior joint capsule. A–D shows posterior knee joint
670 capsule immunohistochemically stained with anti-vimentin antibody. (A) control,
671 (B) IM, (C) RM, and (D) RM + M groups. Arrowheads indicate fibroblasts. Scale
672 bars = 50 μ m. E shows fibroblast number. There was no difference in fibroblast
673 number between the control and IM groups. Compared with those in the control
674 and IM groups, the number of fibroblasts in the RM group increased. In the RM
675 + M group, an increase in fibroblasts was partially attenuated. Values are mean +
676 standard deviation. *: indicates significant difference compared with the control
677 group ($P < 0.05$). †: indicates significant difference compared with the IM group
678 ($P < 0.05$). ‡: indicates significant difference compared with the RM group ($P <$
679 0.05).

680

681 Figure 6: Morphological changes in the posterior knee joint capsule. A–D shows posterior
682 knee joint capsule stained with aldehyde fuchsin-Masson Goldner. (A) control,
683 (B) IM, (C) RM, and (D) RM + M groups. Collagen is stained green. Scale bars

684 = 100 μm . E shows collagen density. There was no difference in collagen density
685 between the control and IM groups. In the RM group, the gaps of collagen bundles
686 narrowed and joint capsules became denser. Consequently, collagen density in the
687 RM group significantly increased compared with the control and IM groups. In
688 the RM + M group, an remobilization-induced increase in collagen density was
689 partially attenuated. Values are mean + standard deviation. *: indicates significant
690 difference compared with the control group ($P < 0.05$). †: indicates significant
691 difference compared with the IM group ($P < 0.05$). ‡: indicates significant
692 difference compared with the RM group ($P < 0.05$).

693

694 Figure 7: Thickness in the posterior joint capsule. A–D shows posterior knee joint capsule
695 stained with aldehyde fuchsin-Masson Goldner. (A) control, (B) IM, (C) RM, and
696 (D) RM + M groups. Up-down arrows indicate posterior joint capsule thickness.
697 Scale bars = 200 μm . E shows joint capsule thickness. Compared with the control
698 group, the posterior joint capsule in the IM group was slightly thickened, but
699 differences were not significant ($P = 0.077$). Joint capsule thickness in the RM
700 group was significantly larger than those in the control and IM groups. In the RM
701 + M group, joint capsule thickness tended to be smaller than in the RM groups (P

702 = 0.067) and was comparable to the IM group. Values are mean + standard
703 deviation. *: indicates significant difference compared with the control group (P
704 < 0.05). †: indicates significant difference compared with the IM group (P < 0.05).